

Discovery of a new *Pseudalomya* Telenga, 1930 (Hymenoptera, Ichneumonidae, Ichneumoninae) species from Taiwan and its implications for the systematic position of this genus

Hsuan-Pu Chen¹, Namiki Kikuchi^{2,3}, Shiu-Feng Shiao¹

1 Department of Entomology, National Taiwan University, No. 1, Sec. 4, Roosevelt Rd., Da'an Dist., Taipei 106, Taiwan **2** Toyohashi Museum of Natural History, 1-238 Oana, Oiwa, Toyohashi, Aichi 441-3147, Japan **3** Systematic Zoology Laboratory, Department of Biological Sciences, Graduate School of Science, Tokyo Metropolitan University, 1-1 Minamiosawa, Hachioji-shi, Tokyo, 192-0397, Japan

Corresponding author: Shiu-Feng Shiao (sfshiao@ntu.edu.tw)

Academic editor: Tamara Spasojevic | Received 25 January 2024 | Accepted 21 March 2024 | Published 9 April 2024

<https://zoobank.org/4C51A1B9-275F-448E-B940-3D544E25B1FE>

Citation: Chen H-P, Kikuchi N, Shiao S-F (2024) Discovery of a new *Pseudalomya* Telenga, 1930 (Hymenoptera, Ichneumonidae, Ichneumoninae) species from Taiwan and its implications for the systematic position of this genus. Journal of Hymenoptera Research 97: 277–296. <https://doi.org/10.3897/jhr.97.119470>

Abstract

The rare genus *Pseudalomya* Telenga comprises two species, which are found only in the Eastern Palaearctic region and high mountains of the Oriental region. The phylogenetic position of *Pseudalomya* remains unclear because of its intermediate morphology between two ichneumonine tribes, Alomyini and Phaeogenini. This article reports the discovery of a new species of *Pseudalomya*: *Pseudalomya truncaticornis* **sp. nov.** Specimens were collected during a survey of insect fauna in the Dasyueshan area of Shei-Pa National Park, one of the high-altitude regions in Taiwan. The new species can be diagnosed by its body coloration, frontal horn shape, facial punctures, metasomal tergite sculpture, and wing venation. To the best of our knowledge, this is the first record of *Pseudalomya* in Taiwan. This article also presents a diagnostic key to the global species of *Pseudalomya*. In this study, molecular phylogenetic analyses were performed using one mitochondrial and two nuclear gene sequences from *P. truncaticornis* **sp. nov.** and other members of the Ichneumoniformes group. The results indicate that *Pseudalomya* should be classified within Phaeogenini, distinct from Alomyini, but more comprehensive phylogenomic studies are needed to confirm this placement.

Keywords

COI, high-altitude, molecular phylogeny, 28S, taxonomy

Introduction

Pseudalomya Telenga, 1930 is a rare genus comprising two valid species: *P. praevara* Telenga, 1930 and *P. nepalensis* Riedel, 2019. Their distribution is restricted to the Eastern Palaearctic region and high mountains of the Oriental region (Yu et al. 2016; Riedel 2019). Another previously described *Pseudalomya* species from Japan – *P. takeii* Kusigemati, 1984 – was later confirmed to be a misidentification of an oxytorine species, *Oxytorus corniger* (Momoi, 1965) (Watanabe 2016).

Because *Pseudalomya* exhibits an intermediate morphology between two ichneumonine tribes Alomyini and Phaeogenini, it has generally been placed in both tribes (Laurenne et al. 2006; Quicke et al. 2009; Tereshkin 2009; Quicke 2015; Riedel 2019). Consequently, the tribal status of *Pseudalomya* remains a topic of debate. On one hand, this genus exhibits similarity with Alomyini because of the following characters: horned frons, enlarged vertex and genae, foramen with genae meeting (or almost meeting) ventrally, oval propodeal spiracle, metasomal tergite II without thyridium, and forewing with the second abscissa of M shorter than the first. On the other hand, *Pseudalomya* also exhibits similarity with Phaeogenini because of the following characters: two-segmented trochanter, two-spurred mid tibia, and metasomal tergite I with spiracles located at apical 0.3 (Laurenne et al. 2006; Tereshkin 2009; Riedel 2019).

Phylogenetic hypotheses reconstructed based on 28S D2–D3 rDNA sequences or combined (morphology and 28S) datasets suggested the tribal placement of *Pseudalomya* within the tribe Phaeogenini (Laurenne et al. 2006; Quicke et al. 2009). Consequently, the morphological similarities between *Pseudalomya* and Alomyini were interpreted as either symplesiomorphic traits or the result of convergent evolution (Quicke 2015). However, because of the lack of sampling of this genus in subsequent comprehensive phylogenetic studies (Bennett et al. 2019; Santos et al. 2021), the phylogenetic position of *Pseudalomya* remains *incertae sedis* (Santos et al. 2021).

In this study, we analyzed three *Pseudalomya* specimens that were newly obtained from the high mountains of central Taiwan. The specimens were collected during fauna inspection for the project SP110113: A survey for the selection of insect indicator species and their microhabitat usage in the Daxueshan area of Shei-Pa National Park. After morphological examinations, these specimens were discovered to be distinct from the known species of *Pseudalomya*. On the basis of morphological evidence, the specimens were subsequently validated as a new species, *Pseudalomya truncaticornis* sp. nov. This article describes the new species and presents a key to the global species of female *Pseudalomya*. In this study, the phylogenetic position of *Pseudalomya* was reassessed through multigene phylogenetic analyses.

Materials and methods

Morphological examination

The morphological terms used in this study were identified from Broad et al. (2018). Measurements were performed with reference to Kikuchi and Konishi (2021). The following abbreviations were used in this study: **OOL**, ocello-ocular line; **POL**, postero-ocellar line; **OD**, ocellar diameter; **PSI**, propodeal spiracle index: major axis of propodeal spiracle/minor axis of propodeal spiracle; **1/M**, the first abscissa of forewing M; **2/M**, the second abscissa of forewing M; **NI**, nervellar index of hindwing: length of hindwing CU between M and cu-a/length of cu-a; **T**, metasomal tergite; **S**, metasomal sternite; and **pS**, posterior section of metasomal sternite.

The measurements in parentheses represent the measurements of the holotype. The cuticular microsculpture is described as per a study conducted by Eady (1968). The whole metasomal sternum was observed and dissected using a method developed by Kikuchi and Konishi (2021). The specimens were examined and measured using a microscope (Leica S8 APO; Leica Microsystems, Wetzlar, Germany) with a micrometer. Photographs were taken using a Leica DMC 5400 camera integrated into a Leica Z16 APO microscope equipped with the auto-stacking system Leica LAS V4.13 (all from Leica Microsystems). Line drawings were generated using Procreate (Savage Interactive, Hobart, Australia). All figures were edited and arranged into figure plates by using Adobe Illustrator CC and Photoshop CC (Adobe Systems, San Jose, CA, USA). The specimens and their photos have been deposited at the following institutes: **NMNS**, National Museum of Natural Science, Taichung, Taiwan; **NARO**, Institute for Agro-Environmental Sciences, National Agriculture and Food Research Organization, Tsukuba, Japan; and **SDEI**, Senckenberg Deutsches Entomologisches Institut, Müncheberg, Germany. The Latin term *ibidem*, meaning “same as previous except as follows,” was abbreviated as “ibid” to abridge information on the location of the materials examined.

Taxon sampling

To reassess the phylogenetic position of *Pseudalomya*, 52 operational taxonomic units (OTUs) from 38 ichneumonine genera were analyzed (Suppl. material 1). In addition, other ichneumonids belonging to the Ichneumoniformes group were included as outgroups (Suppl. material 1). These outgroups were selected from the dataset of Santos (2017) and included 24 species from 23 genera of Cryptinae, 11 species from 11 genera of Phygadeuontinae, one species from one genus of Agriotypinae (*Agriotypus armatus*), and one species from one genus of Microleptinae (*Microleptes splendidulus*). For OTUs whose sequences were obtained from an online database, species identification was double-checked using the Basic Local Alignment Search Tool (BLAST) (Altschul et al. 1990) and the position of preliminary phylogenetic reconstruction. Chimera OTUs were constructed for genera lacking available sequences of multiple markers within individual species.

Molecular data collection and analysis

Total genomic DNA was extracted from the right midleg of each specimen by using a DNeasy Blood and Tissue Kit (Qiagen, Düsseldorf, Germany). Partial sequences of the mitochondrial cytochrome c oxidase I gene (*COI*) and two nuclear genes – D2–D3 regions of 28S ribosomal RNA gene (*28S*) and 18S ribosomal RNA gene (*18S*) – served as molecular markers for phylogenetic reconstruction. The sequences were retrieved from GenBank (National Center for Biotechnology Information). Target sequences were amplified through polymerase chain reaction (PCR). The primer pairs and conditions for PCR are listed in Suppl. material 2. The reaction volume was 15 μL : 5.1 μL of sterile distilled water, 0.6 μL of each (forward/reverse) primer (10 μM), 7.5 μL of GoTaq Green Master Mix (Promega, Madison, WI, USA), and 1.2 μL of DNA template. PCR products were purified and sequenced at Tri-I Biotech (Taipei, Taiwan). Sequences were edited using CodonCode Aligner v.10.0.2 (CodonCode Corporation, Dedham, MA, USA).

MAFFT v.7 (Katoh et al. 2019) was used for automated multiple sequence alignments. The default setting was used for the alignment of *COI*. By contrast, the E-INS-I algorithm was used for the alignment of the two nuclear genes (Santos 2017); the alignments of nuclear markers were manually optimized by removing regions with variable lengths and gaps. The translated alignment of *COI* was checked for stop codons by using MEGA v.11 (Tamura et al. 2021). All newly obtained sequences were uploaded on GenBank. The numbering of positions started from the gene's first nucleotide (full-length *COI* sequences served as references for numbering: GenBank accession [JX131613](#) [*Diadromus collaris*] and [MG923483](#) [*Amblyjoppa* sp.]).

Molecular phylogeny

To infer the phylogenetic position of *Pseudalomya*, phylogeny was reconstructed using the following four datasets: *COI*, *28S*, *18S*, and concatenated *18S+28S+COI*. The concatenated dataset was first partitioned by gene and then, for the protein-coding *COI*, also by codon position (first plus second versus third). ModelFinder (Kalyaanamoorthy et al. 2017) with “partition merging” was used for searching the optimal partitioning scheme and substitution models under the Bayesian Information Criteria.

Maximum likelihood (ML) phylogenetic trees were reconstructed using IQ-TREE v.1.6.12 (Nguyen et al. 2015). This program was accessed through the web server W-IQ-TREE (Trifinopoulos et al. 2016), which is available at <http://iqtree.cibiv.univie.ac.at/>. Ten independent ML searches were performed for the concatenated dataset. After, the tree with the highest likelihood score was selected as the best-topology tree. Nodal support was assessed using the ultrafast bootstrap approximation (UFBoot2) method (Hoang et al. 2017) and SH-like approximate likelihood ratio test (SH-aLRT) (Guindon et al. 2010) under the default setting for the ML method. Nodes with an SH-aLRT value of $\geq 80\%$ and a UFBoot value of $\geq 95\%$ were considered to have strong support. For further interpretation of the tribal placement of *Pseudalomya*, the tribal classification system described by Santos et al. (2021) was applied herein.

Results

Taxonomy

Subfamily Ichneumoninae Latreille, 1802

Genus *Pseudalomya* Telenga, 1930

Pseudalomya Telenga, 1930: 107. Type: *Pseudalomya praevara* Telenga, 1930, by original monotypy.

Pseudalomya truncaticornis Chen & Kikuchi, sp. nov.

<https://zoobank.org/5C674A42-79DA-410C-A52C-25191684E0F6>

Figs 1–4

Diagnosis. This species can be distinguished from other congeners in having the following combination of characters: frontal horn short and apically truncated; face sparsely punctate; metasomal tergites smooth with sparse and minute punctures; forewing with 1cu-a distad to M&RS; head reddish brown; mesosoma and legs black; and metasomal tergites metallic-blue.

Material examined. Holotype. TAIWAN • 1♀; Miaoli County, Tai'an Township, Shei-Pa National Park, Mt. Huoshi; 24°22'47.78"N, 121°10'53.67"E (DMS); alt. 3160 m; 25 Aug. 2021–12 May. 2022; Jung-Chang Chen, Kuang-Yao Chen, Li-Jen Chang, Ta-Hsiang Li and Hung-Yang Shen leg.; Malaise Trap; GenBank: [PP175350](#) (COI), [PP188485](#) (28S), [PP188484](#) (18S); Sample ID: SP0060; Voucher: NMNS ENT 8836-1.

Paratypes. TAIWAN • 2♀; *ibid*; GenBank: [PP175351](#) (COI, SP0061), [PP175352](#) (COI, SP0062); Sample ID: SP0061–SP0062; Voucher: NARO (SP0061); NMNS ENT 8836-2 (SP0062).

Description. Female. Head: 1.43–1.75 (1.75)× as wide as deep; antenna with 26–27 (27) flagellomeres; first flagellomere 1.13–1.22 (1.13)× as long as wide and 1.04–1.12 (1.04)× as long as second one; second flagellomere 1.08–1.19 (1.08)× as long as wide, remaining flagellomeres about 1.0× as long as wide; frons strongly and transversely striated; horn laterally depressed, apically truncated or slightly rounded (Figs 2A, 4A); face polished, 2.16–2.43 (2.16)× as wide as long, sparsely punctate (distance between punctures 2.0–3.0× average puncture diameter) in middle and relatively dense (distance 1.0–2.0× average puncture diameter) laterally (Figs 2B, 4C), with setae; eyes bare, frontal orbit elevated; clypeus polished, 2.25–2.88 (2.88)× as wide as long, sparsely punctate with long setae, rounded in ventral margin and flat in lateral view (Figs 2A, B, 4C, F); malar space 1.29–1.73 (1.73)× as basal width of mandible, smooth in dorsal half and densely coriaceous in ventral half (Figs 2A, B, 4C); mandible unidentate, rounded apically, broad, flat, polished and punctate with long setae at

base (Fig. 4C); gena polished and sparsely punctate (Fig. 2C), pointed and strongly narrowed ventrally, meeting under the foramen; ocellar area and vertex rugose, rugose-punctate laterally; $POL/OD=1.20-1.50$ (1.50), $OOL/OD=2.20-2.54$ (2.36) (Figs 2A, 4E); occiput smooth; occipital carina strong and complete, genal carina meeting hypostomal carina far from mandible base at ventral tip of genae in $1.40-1.73$ (1.73) \times of basal width of mandible.

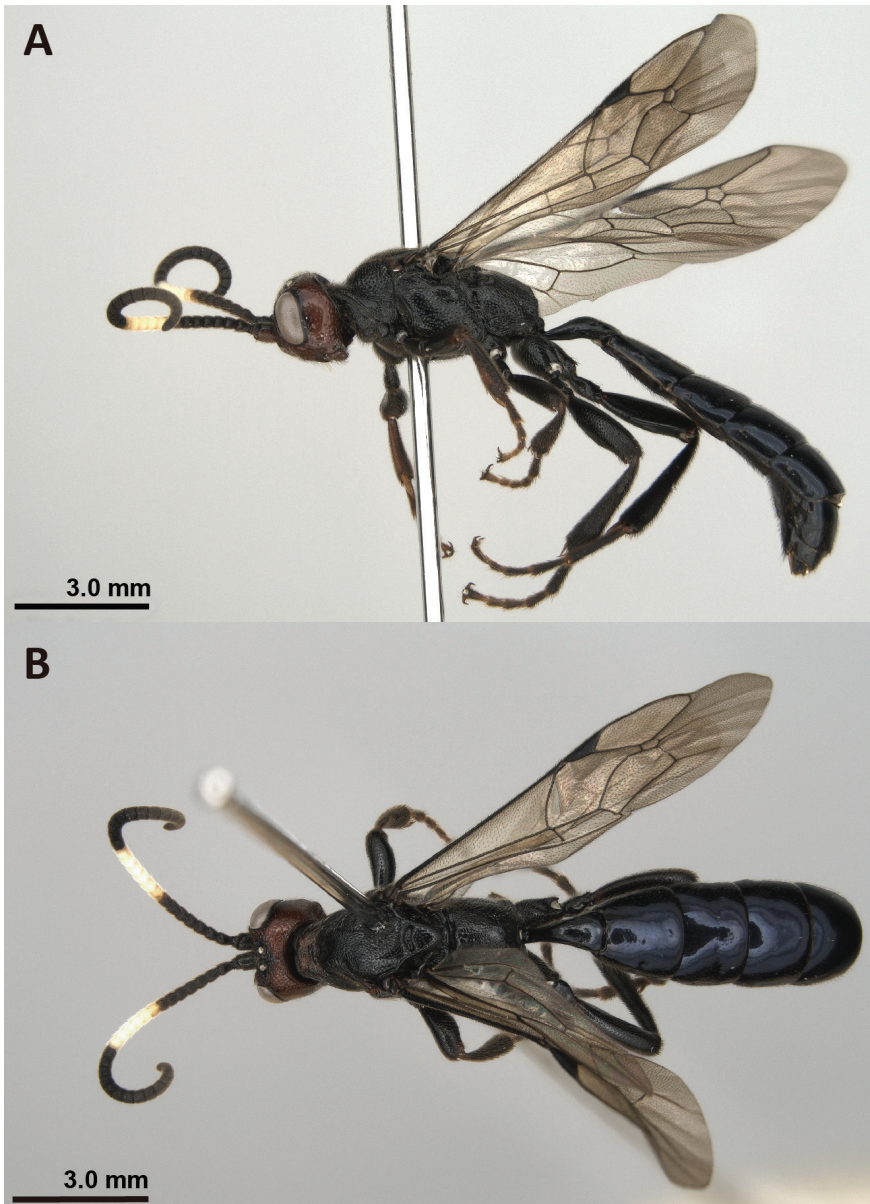


Figure 1. *Pseudalomya truncaticornis* sp. nov. holotype (NMNS ENT 8836-1) **A** lateral view of the habitus **B** dorsal view of the habitus. Photographed by Hsuan-Pu Chen.

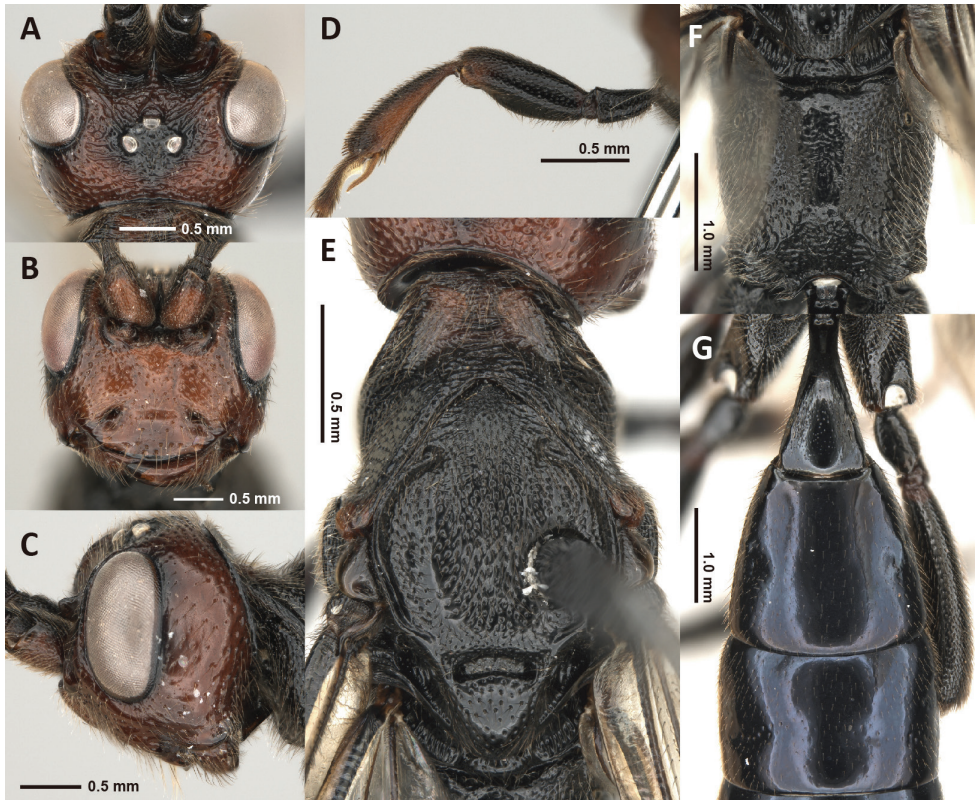


Figure 2. *Pseudalomya truncaticornis* sp. nov. holotype (NMNS ENT 8836-1) **A** dorsal view of the head **B** anterior view of the head **C** lateral view of the head **D** foreleg **E** dorsal view of the mesoscutum **F** dorsal view of the propodeum **G** dorsal view of the metasomal tergites. Photographed by Hsuan-Pu Chen.

Mesosoma: polished; pronotum with setae, transversely and strongly strigose dorsally, evenly and coarsely punctate dorsolaterally, and rugose-punctate ventrolaterally (Figs 2E, 3A); epomia present; propleuron coarsely punctate with setae; mesoscutum flat, 1.15–1.21 (1.21) \times as long as wide, with median lobe densely and coarsely punctate, lateral lobes evenly punctate but polished and sparsely punctate posteriorly, with setae (Fig. 2E); notauli present anteriorly; scutellum flat, 1.09–1.18 (1.18) \times as long as wide, sparsely punctate with setae, lateral carina absent (Fig. 2E); mesopleuron punctate, but rugose in dorso-anterior corner and middle posterior 0.5–0.8 (0.5), with mesopleural sulcus and furrow crenulate (Fig. 3A); epicnemial carina complete, extend to whole height of mesopleuron; sternaulus present in anterior 0.4 of mesopleuron; mesepisternum smooth; metapleuron evenly and coarsely punctate with setae in upper division and dorsal half, strongly and transversely strigose in ventral half; propodeal spiracle oval, 1.43–1.57 (1.43) \times as long as wide; posterior transverse carina of mesosternum interrupted anterior to mid-coxa; propodeum evenly and coarsely punctate with setae, with area basalis smooth, area superomedia and area petiolaris rugose-punctate, and area postero-externa rugose-foveolate (Fig. 2F); juxtacoxal carina present in

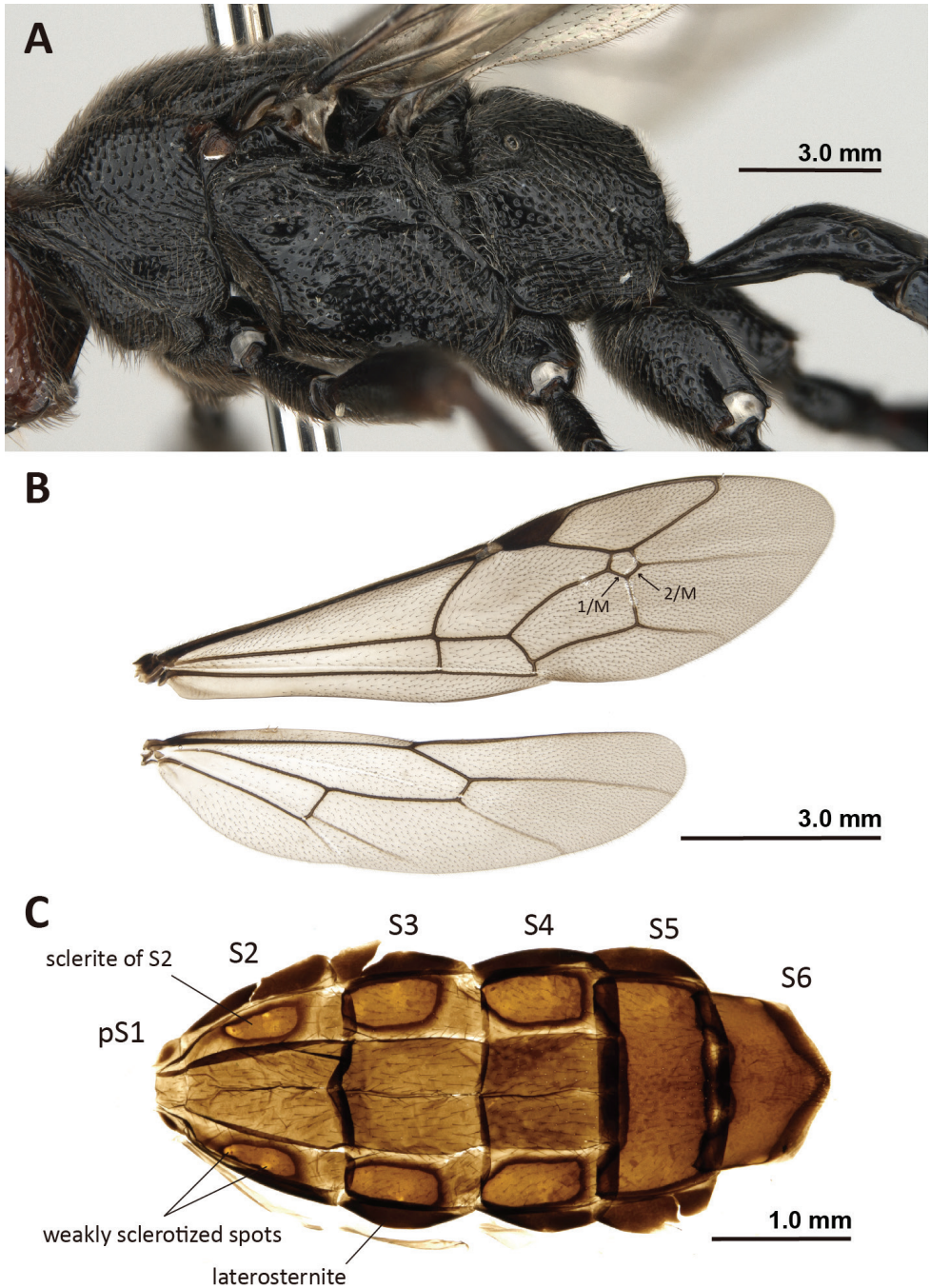


Figure 3. *Pseudalomya truncaticornis* sp. nov., NMNS ENT 8836-1 (A), NMNS ENT 8836-2 (B), and NARO (C) A lateral view of the mesosoma B wings C metasomal sternites. Photographed by Hsuan-Pu Chen (A, B) and Namiki Kikuchi (C).

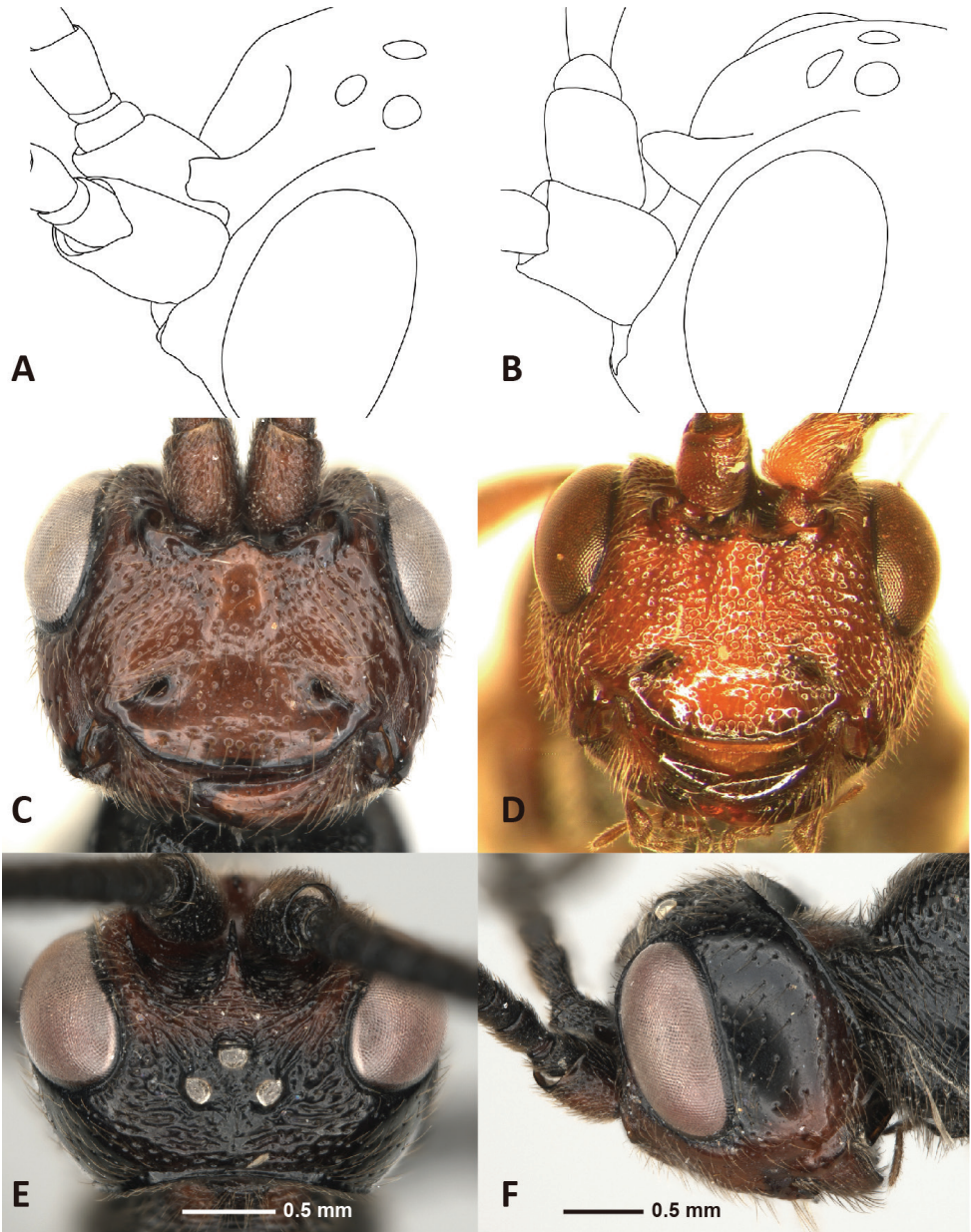


Figure 4. Characters of two *Pseudalomya* species. Frontal horns: **A** *Pseudalomya truncaticornis* sp. nov. (holotype, NMNS ENT 8836-1) **B** *Pseudalomya nepalensis* (holotype, SDEI). Faces: **C** *P. truncaticornis* sp. nov. (holotype, NMNS ENT 8836-1) **D** *P. nepalensis* (holotype, SDEI) **E** darker specimen of *P. truncaticornis* sp. nov. (paratype, NMNS ENT 8836-2), dorsal view of the head **F** darker specimen of *P. truncaticornis* sp. nov. (paratype, NMNS ENT 8836-2), lateral view of the head. Illustrated and photographed by Hsuan-Pu Chen (**A–C, E, F**) and Matthias Riedel (**D**).

basal 0.6; pleural and submetapleural carina present basally; lateromedian longitudinal carina weak; lateral longitudinal carina, anterior transverse carina, and propodeal apophysis absent; posterior transverse carina present, but weak medially.

Legs: evenly punctate with setae; coxa smooth dorso-apically; fore femur 2.63–2.84 (2.74)× as long as wide; hind femur 3.23–3.34 (3.34)× as long as wide, 0.21–0.24 (0.21)× as long as hind tibia; hind first tarsomere 1.75–1.92 (1.92)× as long as second tarsomere, and 0.45–0.49 (0.45)× as long as hind tibia; tibial spurs 2; tarsal claws normal.

Wings: forewings narrowed, 3.80–4.22 (4.12)× as long as wide, and length 8.01–8.45 (8.45) mm (Fig. 3B); forewing 1cu-a postfurcal, distad M & RS 0.23–0.33 (0.33)× by its length; areolet pentagonal, truncate anteriorly, with 2rs-m 1.10–1.26 (1.16)× as long as 3rs-m, and 1/M 1.05–1.14× as long as 2/M; 2 m-cu with two bulla; hindwing hamuli 7–9 (9), NI = 3.52–4.29 (4.29), CU and AA after cu-a weak.

Metasoma: polished; T1 2.00–2.68 (2.01)× as long as its apical width, smooth, postpetiole sparsely and minutely punctate (Fig. 2G); spiracles of T1 located at about 0.7 of length of tergite (Fig. 3A); T2 0.91–0.95 (0.91)× as long as its apical width, with gastrocoeli and thyridium absent (Fig. 2G); T3 0.63–0.72 (0.63)× as long as its apical width; tergites after T1 smooth with sparse and minute puncture (Fig. 2G); pS1 and S2 separated by weak crease (Fig. 3C); laterosternites strongly sclerotized in S1–5, separately from median sternites by crease; median sternites strongly sclerotized, with weakly sclerotized median area in S2–4 and separated by creases; sclerites of S2 0.5× as long as S2, not touched its posterior margin, with two weakly sclerotized spots; median sternites of S5 and S6 complete; metasomal apex amblypygous (Fig. 1A), with apical margin of hypopygium pointed (Fig. 3C); ovipositor sheath 0.16–0.20 (0.17)× as long as hind tibia, smooth with setae; ovipositor with upper valve slightly longer than lower valve, and lower valve with fine teeth.

Coloration: head mainly reddish brown, except central area of frons, horn, orbits, ventral margin of gena and clypeus, face below antennal sockets and around tentorial pits, ocellar area, apical half of mandible, occiput except its dorsal margin, and occipital carina black (Fig. 2A–C); antenna mainly black except flagellomeres 8 (or 9)–13 ivory and ventral surface of scape reddish brown (Fig. 1A, B); mesosoma mainly black, except two stripes at dorsal surface of pronotum, posterior corner of pronotum, and postspiracular sclerite before tegula reddish brown (Figs 1A, B, 2E, 3A); metasomal tergites metallic dark blue (Fig. 2G), with sternites black tinged with reddish brown; ovipositor sheaths black and ovipositor reddish brown; legs mainly black except apical fore femur, ventral side of fore tibia, basal and apical basitarsus, apical tarsomeres reddish brown (Fig. 1A); wings tinged with infusate, with veins and pterostigma black (Fig. 3B). One specimen (NMNS ENT 8836-2; SP0062) with temple above eyes, whole occiput, and all legs black (Fig. 4E, F).

Male. Unknown.

Etymology. The specific name “*truncaticornis*” is derived from the Latin “*truncati-*” (meaning “maimed” or “having appendages cut off”) plus “*cornis*” (meaning “horned”). It refers to the truncated apex of the horn on the frons in this species. Name is an adjective.

Distribution. Taiwan.

Bionomics. Host and phenology unknown. The specimens were collected from Taiwan Hemlock (*Tsuga chinensis*) (Pinaceae) forest in the high-altitude area (alt. 3160 m) of central Taiwan, with *Yushania niitakayamensis* (Bambusoideae, Poaceae), *Rhododendron* species (Ericaceae), and moss as ground-cover plants (Fig. 5).

Remarks. Comparisons of the photos of holotypes and descriptions of congener species revealed the highest level of similarity between *P. truncaticornis* sp. nov. and *P. nepalensis* Riedel, 2019. However, unlike *P. nepalensis*, the new species had the black coloration in mesosoma and legs (reddish brown in *P. nepalensis*), the middle of face with sparse punctures with distance between punctures 2.0–3.0× their diameter (dense in *P. nepalensis*, distance less than 1.0× their diameter), and a short and apically truncated frontal horn (long and apically rounded in *P. nepalensis*). While variation in the color of the head was observed within *P. truncaticornis* sp. nov., given the disjunct geographical distributions between *P. truncaticornis* sp. nov. and *P. nepalensis* (Taiwan and the Himalaya, respectively) and the presence of morphological differences beyond mere coloration, *P. truncaticornis* sp. nov. is considered a distinct species. To the best of our knowledge, this is the first record of *Pseudalomya* in Taiwan.



Figure 5. Habitat of *Pseudalomya truncaticornis* sp. nov. in Mount Huoshi (24°22'47.78"N, 121°10'53.67"E DMS), Shei-Pa National Park. Photographed by Ta-Hsiang Lee.

Key to world species of female *Pseudalomya* Telenga, 1930

- 1 Metasomal tergites not smooth, with postpetiole of T1 rugose, and T2 coriaceous; Forewing 1cu-a interstitial, opposite to M&RS; metasomal tergites not metallic-blue..... ***P. praevara* Telenga, 1930**
- Metasomal tergites smooth (Figs 1B, 2G); Forewing 1cu-a postfurcal, distad to M&RS (Fig. 3B); tergites metallic-blue (Figs 1B, 2G) **2**
- 2 Frontal horn long, rounded apically (Fig. 4B); punctures separated by less than 1.0× their diameter in middle of face (Fig. 4D); mesosoma and legs almost reddish brown..... ***P. nepalensis* Riedel, 2019**
- Frontal horn short, truncated apically (Fig. 4A); punctures separated by 2.0–3.0× their diameter in middle of face (Figs 2B, 4C); mesosoma and legs black (Fig. 1A, B)..... ***P. truncaticornis* sp. nov.**

Molecular dataset

The dataset for molecular phylogeny comprised six newly obtained sequences: three *COI* sequences from the ichneumonine species *Quandrus pepsoides* (Smith, 1852), *Callajoppa exaltatoria* (Panzer, 1804), and *Holcojoppa bicolor* (Radoszkowski, 1887) and one sequence each of *COI*, *28S*, and *18S* from *P. truncaticornis* sp. nov.. In addition, the dataset included 250 sequences – 83 *COI*, 88 *28S*, and 79 *18S* sequences – from GenBank (Suppl. material 1).

No pseudogene, identifiable by the occurrence of stop codons in translated (amino acid) sequences, was detected in the protein-coding gene dataset. However, one *18S* sequence from *Pseudoplatylabus apicalis* (GenBank accession [KU753140](#)) was eliminated because of its abnormal genetic distance in the *18S* gene tree pretest. Table 1 presents the basic details of each aligned dataset. The information presented in this table includes the average length of unaligned sequences, length of aligned sequences, number of variable and parsimony-informative sites, and percentage of GC content. The datasets for the concatenated and individual markers are presented in Suppl. material 3.

Molecular phylogeny

Figs 6, 7 depict the ML phylogenetic trees reconstructed using the concatenated *18S+28S+COI* dataset and the *COI* and *28S* datasets, respectively. The *18S* gene tree

Table 1. Summary of each aligned and trimmed molecular dataset. The table presents information on the average length of unaligned sequences, length of aligned sequences, number of variable and parsimony-informative (Pars-Inf) sites, and percentage of GC content.

	Number of sequences	Average length	Aligned length	Variable sites	Pars-Inf sites	GC (%)
<i>COI</i>	87	638.8	648	414	351	27.7
<i>28S</i>	89	613.3	625	283	169	59.7
<i>18S</i>	79	890.9	1302	70	31	49.5
<i>18S+28S+COI</i>	89	2028.6	2575	767	551	45.9

could not satisfactorily resolve the phylogenetic relationships in the Ichneumoniformes group (see Suppl. material 4: fig. S3). All trees were rerooted using the outgroup *Agriotypus armatus* (Agriotypinae). The complete phylogenetic trees resulting from all datasets are presented in Suppl. material 4.

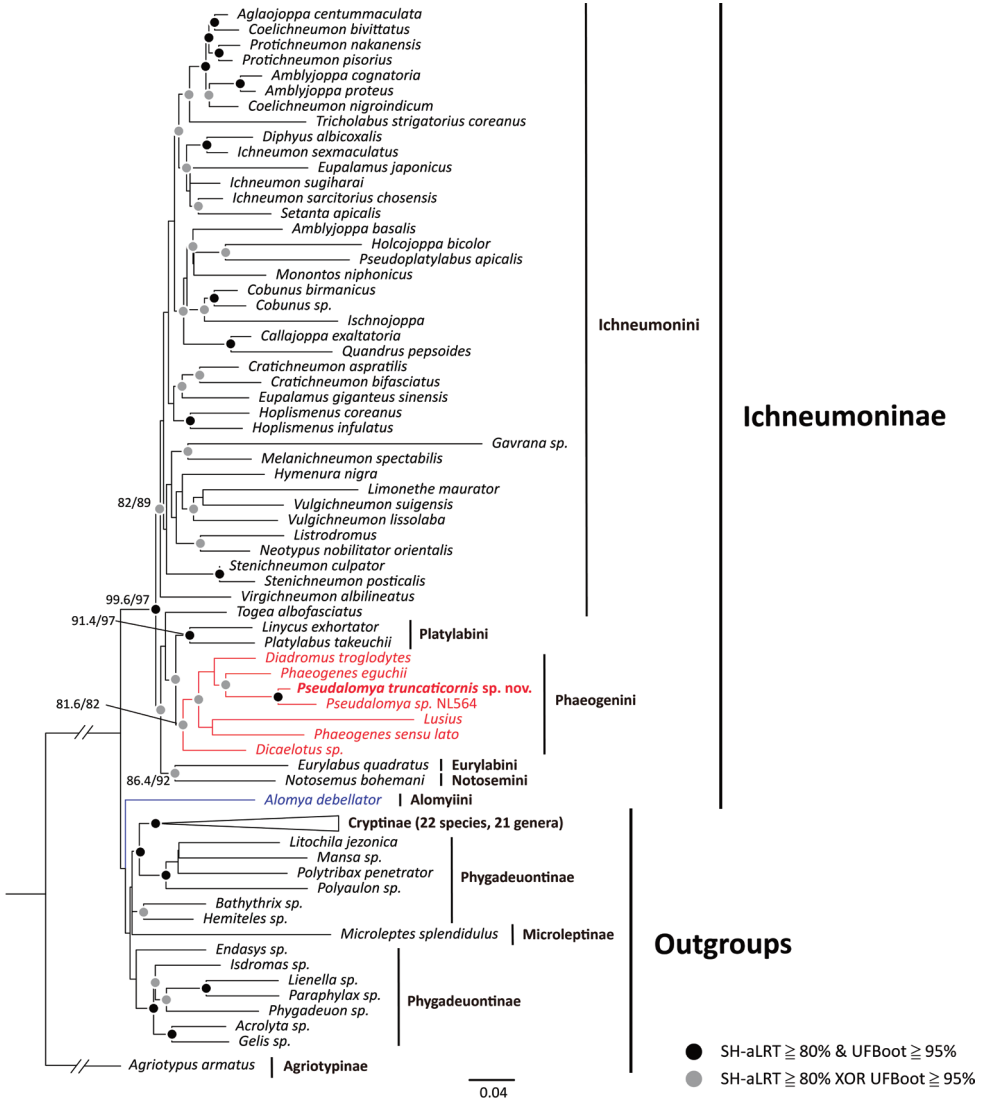


Figure 6. Maximum likelihood phylogenetic tree of Ichneumoninae reconstructed using the concatenated *18S+28S+COI* dataset (2575 bp; *18S*: 1302 bp; *28S*: 625 bp; *COI*: 648 bp; SYM+I+G4 [1–1302, 1303–1927, 1928–2575\3, and 1929–2575\3 bp]; HKY+F+I+G4 [1930–2575\3 bp]). The red and blue colors indicate Phaeogenini and Alomyiini, respectively. Branch lengths of the phylogenetic tree are proportional to the infer number of nucleotide substitutions per site, except for the branch of the outgroup *Agriotypus armatus*. Circles on the nodes indicate different SH-aLRT/UFBoot values. Nodal support with an SH-aLRT value of <80% and a UFBoot value of <95% is not shown. Abbreviations: SH-aLRT, SH-like approximate likelihood ratio test; UFBoot, ultrafast bootstrap approximation; XOR, one or the other but not both.

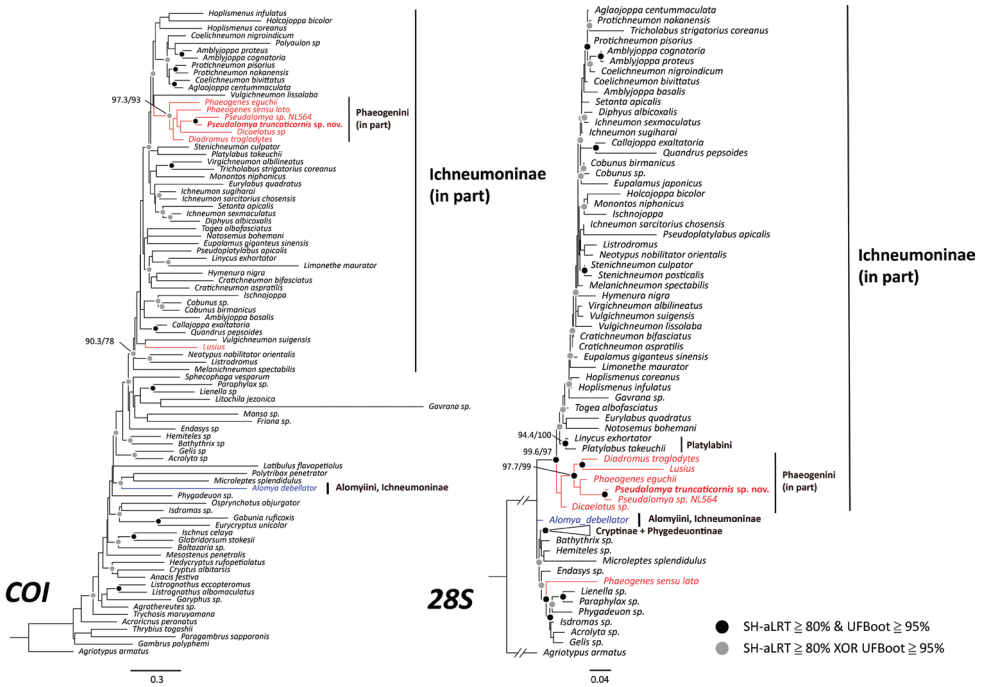


Figure 7. Maximum likelihood phylogenetic trees of Ichneumoninae reconstructed using the *COI* and *28S* datasets (*COI*: 648 bp; GTR+F+I+G4 [1–648\3 and 2–648\3 bp]; HKY+F+I+G4 [3–648\3 bp]; *28S*: 625 bp; GTR+F+I+G4 [1–625 bp]). The red and blue colors indicate Phaeogenini and Alomyini, respectively. Branch lengths of the phylogenetic trees are proportional to the infer number of nucleotide substitutions per site, except for the branch of the outgroup *Agriotypus armatus*. Circles on the nodes indicate different SH-aLRT/UFBoot values. Nodal support with an SH-aLRT value of <80% and a UF-Boot value of <95% is not shown. Abbreviations: SH-aLRT, SH-like approximate likelihood ratio test; UFBoot, ultrafast bootstrap approximation; XOR, one or the other but not both.

In the tree reconstructed using the concatenated dataset, the subfamily Ichneumoninae excluding *Alomya debellator* (tribe: Alomyini), is recovered as a strongly supported clade (SH-aLRT/UFBoot = 99.6/97) and sister to the clade including Alomyini, Microleptinae, Cryptinae, and Phygadeuontinae (Fig. 6). *A. debellator* is sister to the clade including Microleptinae, Cryptinae, and Phygadeuontinae (low nodal support; SH-aLRT/UFBoot = 70.1/78) but was not a member of the Ichneumoninae. The ichneumonine tribes proposed by Santos et al. (2021) are recovered as monophyletic groups, with the exception of Ichneumonini; *Togea albofasciatus* was nested within the clade including Notosemini, Eurylabini, Platylabini, and Phaeogenini. However, with the exception of Platylabini (SH-aLRT/UFBoot = 91.4/97), none of the sampled tribes were strongly supported (SH-aLRT/UFBoot = 81.6/82 in Phaeogenini and 86.4/92 in the clade including Notosemini and Eurylabini). Finally, *Pseudalomya* is recovered as a member of Phaeogenini, distinct from Alomyini (Fig. 6); however, the sister relationship of the new species with *Phaeogenes eguchii* was not strongly supported (SH-aLRT/UFBoot = 52.2/95).

In the gene tree reconstructed using *COI*, *Pseudalomya* is recovered in the phaeogenine clade excluding *Lusius* (SH-aLRT/UFBoot = 97.3/93); in the tree reconstructed using *28S*, *Pseudalomya* is recovered in the strongly supported phaeogenine clade excluding *Phaeogenes sensu lato* and *Dicaelotus* sp. (SH-aLRT/UFBoot = 97.7/99; Fig. 7). Notably, neither tree indicates *A. debellator* as a member of the Ichneumoninae. Neither Ichneumoninae nor ichneumonine tribes are recovered as strongly supported monophyletic groups in either tree. However, Platylabini is recovered as a strongly supported monophyletic group in the *28S* tree (SH-aLRT/UFBoot = 94.4/100; Fig. 7).

Discussion

The genus *Pseudalomya* has been sampled in previous phylogenies reconstructed by *28S* data (Laurenne et al. 2006) or combined (*28S* + morphology) data (Quicke et al. 2009). Both hypotheses supported the placement of *Pseudalomya* within Phaeogenini. To the best of our knowledge, our study is the first to present *COI*-based and multigene molecular phylogeny that includes *Pseudalomya*. The results support the placement of *Pseudalomya* within Phaeogenini. However, the precise relationship of *Pseudalomya* with other members of Phaeogenini as reported in the literature and the present study differs because of between-study differences in taxon sampling and methodology. *Pseudalomya* was shown sister to *Tycherus* in the study of Laurenne et al. (2006), to an unidentified phaeogenine genus in the study of Quicke et al. (2009), to *Dicaelotus* sp. in our *COI*-based phylogenetic analysis (Fig. 7), and to *Phaeogenes eguchii* in our *28S*-based and concatenated multigene phylogenetic analyses (Figs 6, 7). The aforementioned relationships are not highly supported, with the exception of that reported in Laurenne et al. (2006).

In our study, the Alomyini (*Alomya debellator*) is not recovered as a member of Ichneumoninae; this finding is congruent with the *28S*-based hypothesis proposed by Laurenne et al. (2006) but incongruent with phylogenetic hypotheses reconstructed using morphological data (Gokhman 1992, 1995), combined morphological and multigene data (Quick et al. 2009; Bennett et al. 2019), or genomic data (Santos et al. 2021).

Our findings, which were derived from phylogenetic analyses performed using universal genetic markers via Sanger sequencing, unveiled incongruent phylogenetic relationships within Ichneumoninae (Figs 6, 7). The tree reconstructed using the *18S* dataset even failed to reveal subfamily-level relationships, likely because of to the conservativeness of this marker (see Suppl. material 4: fig. S3). These results imply probable constraints in phylogenetic inference using a restricted set of Sanger-based genetic markers or involving incomprehensive taxon sampling. However, our results do distinctly demonstrate the position of *Pseudalomya* as not belonging to Alomyini and clustered within Phaeogenini. Additionally, the alignment of *COI* sequences revealed that *Pseudalomya* lacked a unique insertion sequence (nucleotides 403–408) specific to *Alomya* (see Suppl. material 3: pseudalomya_ichneumoniformes_coi_withreference.fas), providing an additional character for differentiating between *Pseudalomya* and Alomyi-

ni (at least *Alomya*). Considering the discrepancies between the literature and our study regarding the limitations of Sanger-based phylogenetic analyses, we refrained from the tribal reclassification of *Pseudalomya*. Comprehensive phylogenetic analyses based on genomic data are required to accurately determine the tribal status of *Pseudalomya*.

Lastly, this study indicates that the distribution of *Pseudalomya* extends from the Eastern Palaearctic region (Russia, Korea) and the Himalayas (Nepal) to Taiwan. The oriental species of *Pseudalomya* – *P. nepalensis* and *P. truncaticornis* sp. nov. – exhibit disjunct distributions between the Himalayas and Taiwan. This unique distribution pattern is also observed in vascular plants, vertebrates, and insects (e.g., Hsu and Yen 1997; Päckert et al. 2012; Niu et al. 2018). This pattern may be explained by long-distance dispersal, postglacial contraction, limited faunistic studies in the high-altitude intermediate regions, or the lack of material examined (Yen et al. 2000; Wang et al. 2013; Niu et al. 2018). Thus, further studies are required to comprehensively clarify the distribution of *Pseudalomya*.

Funding

This study was funded by Taiwan's National Science and Technology Council [grant to the corresponding author: 111-2621-B-002-002] and Bureau of Animal and Plant Health Inspection and Quarantine [grants to the corresponding author: 111AS-5.3.3-BQ-B2(2), 112AS-5.3.3-BQ-B2(2), and 112-RA-BQ-01(Z)].

Competing interests

The authors have declared that no competing interests exist.

Acknowledgments

We would like to express our sincere thanks to Matthias Riedel (Zoologische Staatssammlung München, Bad Fallingb., Germany) for providing the holotype photos of *Pseudalomya nepalensis*; Yun Hsiao (Institute of Ecology and Evolutionary Biology, National Taiwan University, Taipei, Taiwan) for assisting in phylogenetic analyses; Yu-Feng Hsu, Yu-Ming Hsu, and Kuang-Yao Chen (Department of Life Science, National Taiwan Normal University, Taipei, Taiwan), and Jung-Chang Chen, Li-Jen Chang, Ta-Hsiang Li, and Hung-Yang Shen for providing the specimens and collecting under the project SP110113 (“A survey for selection of insect indicator species and their microhabitat usage in the Daxueshan area of Shei-Pa National Park”); and two reviewers, Brandon Claridge (Utah State University, Logan, USA) and Davide Dal Pos (Department of Biology, University of Central Florida, Orlando, USA), for providing constructive feedback that improved the quality of our manuscript.

References

- Altschul SF, Gish W, Miller W, Myers EW, Lipman DJ (1990) Basic local alignment search tool. *Journal of Molecular Biology* 215: 403–410. [https://doi.org/10.1016/S0022-2836\(05\)80360-2](https://doi.org/10.1016/S0022-2836(05)80360-2)
- Bennett AM, Cardinal S, Gauld ID, Wahl DB (2019) Phylogeny of the subfamilies of Ichneumonidae (Hymenoptera). *Journal of Hymenoptera Research* 71: 1–156. <https://doi.org/10.3897/jhr.71.32375>
- Broad GR, Shaw MR, Fitton MG (2018) Ichneumonid Wasps (Hymenoptera: Ichneumonidae): their classification and biology. *Handbooks for the identification of the British insects* 7(12): 1–418.
- Eady RD (1968) Some illustrations of microsculpture in the Hymenoptera. *Proceedings of the Royal Entomological Society of London* 43: 66–72. <https://doi.org/10.1111/j.1365-3032.1968.tb01029.x>
- Gokhman VE (1992) On the origin of endoparasitism in the subfamily Ichneumoninae (Hym., Ichneumonidae). *Zhurnal Obshchei Biologii* 53: 600–608.
- Gokhman VE (1995) Trends of biological evolution in the subfamily Ichneumoninae and related groups (Hymenoptera, Ichneumonidae): an attempt of phylogenetic reconstruction. *Russian Entomological Journal* 4: 91–103.
- Guindon S, Dufayard J-F, Lefort V, Anisimova M, Hordijk W, Gascuel O (2010) New algorithms and methods to estimate maximum-likelihood phylogenies: Assessing the performance of PhyML 3.0. *Systematic Biology* 59(3): 307–321. <https://doi.org/10.1093/sysbio/syq010>
- Hoang DT, Chernomor O, von Haeseler A, Minh BQ, Vinh LS (2017) UFboot2: Improving the Ultrafast Bootstrap Approximation. *Molecular Biology and Evolution* 35 (2): 518–522. <https://doi.org/10.1093/molbev/msx281>
- Hsu YF, Yen SH (1997) Notes on *Boloria pales yangi*, ssp. nov., a remarkable disjunction in butterfly biogeography (Lepidoptera: Nymphalidae). *Journal of Research on the Lepidoptera* 34: 142–146. <https://doi.org/10.5962/p.266565>
- Kalyaanamoorthy S, Minh BQ, Wong TKF, von Haeseler A, Jermin LS (2017) Modelfinder: Fast model selection for accurate phylogenetic estimates. *Nature Methods* 14: 587–589. <https://doi.org/10.1038/nmeth.4285>
- Katoh K, Rozewicki J, Yamada KD (2019) MAFFT online service: Multiple sequence alignment, interactive sequence choice and visualization. *Briefings in Bioinformatics* 20 (4): 1160–1166. <https://doi.org/10.1093/bib/bbx108>
- Kikuchi N, Konishi K (2021) A taxonomic revision of the genus *Linyctus* Cameron, 1903 from Japan. *Zootaxa* 4948(4): 546–558. <https://doi.org/10.11646/zootaxa.4948.4.3>
- Laurenne NM, Broad G, Quicke DLJ (2006) Direct optimization and multiple alignment of 28S D2–D3 rDNA sequences: problems with indels on the way to a molecular phylogeny of the cryptine ichneumon wasps (Insecta: Hymenoptera). *Cladistics* 22: 442–473. <https://doi.org/10.1111/j.1096-0031.2006.00112.x>
- Nguyen LT, Schmidt HA, von Haeseler A, Minh BQ (2015) IQ-TREE: a fast and effective stochastic algorithm for estimating maximum-likelihood phylogenies. *Molecular Biology and Evolution* 32(1): 268–274. <https://doi.org/10.1093/molbev/msu300>

- Niu Y-T, Ye J-F, Zhang J-L, Wan J-Z, Yang T, Wei X-X, Lu L-M, Li J-H, Chen Z-D (2018) Long-distance dispersal or postglacial contraction? Insights into disjunction between Himalaya–Hengduan Mountains and Taiwan in a cold-adapted herbaceous genus, *Triplostegia*. *Ecology and Evolution* 8: 1131–1146. <https://doi.org/10.1002/ece3.3719>
- Päckert M, Martens J, Sun YH, Severinghaus LL, Nazarenko AA, Ting J, Töpfer T, Tietze DT (2012) Horizontal and elevational phylogeographic patterns of Himalayan and Southeast Asian forest passerines (Aves: Passeriformes). *Journal of Biogeography* 39: 556–573. <https://doi.org/10.1111/j.1365-2699.2011.02606.x>
- Quicke DLJ (2015) The braconid and ichneumonid parasitoid wasps: biology, systematics, evolution and ecology. John Wiley & Sons (West Sussex), 704 pp. <https://doi.org/10.1002/9781118907085>
- Quicke DLJ, Laurence NM, Fitton MG, Broad GR (2009) A thousand and one wasps: a 28S rDNA and morphological phylogeny of the Ichneumonidae (Insecta: Hymenoptera) with an investigation into alignment parameter space and elision. *Journal of Natural History* 43 (23–24): 1305–1421. <https://doi.org/10.1080/00222930902807783>
- Riedel M (2019) Contribution to the Ichneumoninae (Hymenoptera, Ichneumonidae) of Nepal. *Linzer Biologische Beiträge* 51: 1119–1162.
- Santos BF (2017) Phylogeny and reclassification of Cryptini (Hymenoptera, Ichneumonidae, Cryptinae), with implications for ichneumonid higher-level classification. *Systematic Entomology* 42: 650–676. <https://doi.org/10.1111/syen.12238>
- Santos BF, Wahl DB, Rousse P, Bennett AMR, Kula R, Brady SG (2021) Phylogenomics of Ichneumoninae (Hymenoptera, Ichneumonidae) reveals pervasive morphological convergence and the shortcomings of previous classifications. *Systematic Entomology* 46: 704–724. <https://doi.org/10.1111/syen.12484>
- Tamura K, Stecher G, Kumar S (2021) MEGA11: Molecular Evolutionary Genetics Analysis Version 11. *Molecular Biology and Evolution* 38 (7): 3022–3027. <https://doi.org/10.1093/molbev/msab120>
- Telenga NA (1930) Einige neue Ichneumoniden-Arten aus USSR. *Revue Russe d'Entom* 24: 104–108.
- Tereshkin AM (2009) Illustrated key to the tribes of subfamilia Ichneumoninae and genera of the tribe Platylabini of world fauna (Hymenoptera, Ichneumonidae). *Linzer Biologische Beiträge* 41(2): 1317–1608.
- Trifinopoulos J, Nguyen LT, von Haeseler A, Minh BQ (2016) W-IQ-TREE: a fast online phylogenetic tool for maximum likelihood analysis. *Nucleic Acids Research* 44(W1): W232–W235. <https://doi.org/10.1093/nar/gkw256>
- Wang WJ, McKay BD, Dai CY, Zhao N, Zhang RY, Qu YH, Song G, Li SH, Liang W, Yang XJ, Pasquet E, Lei FM (2013) Glacial expansion and diversification of an East Asian montane bird, the green-backed tit (*Parus monticolus*). *Journal of Biogeography* 40: 1156–1169. <https://doi.org/10.1111/jbi.12055>
- Watanabe K (2016) Taxonomic Position of *Pseudalomya takeii* Kusigemati, 1984 (Hymenoptera: Ichneumonidae), with a New Synonym. *Japanese Journal of Systematic Entomology* 22(1): 35–36.

Yen SH, Nässig WA, Naumann S, Brechlin R (2000) A new species of the *miranda*-group of the genus *Loepa* from Taiwan (Lepidoptera: Saturniidae). *Nachrichten des Entomologischen Vereins Apollo* 21: 153–162.

Yu DSK, van Achterberg C, Horstmann K (2012) *Taxapad 2012, Ichneumonoidea 2011*. Ottawa, Ontario. <http://www.taxapad.com> [database on flash-drive]

Supplementary material 1

Sequences used in this study

Authors: Hsuan-Pu Chen, Namiki Kikuchi

Data type: xlsx

Explanation note: The cells in blue with bold font indicate the newly obtained sequences in this study.

Copyright notice: This dataset is made available under the Open Database License (<http://opendatacommons.org/licenses/odbl/1.0/>). The Open Database License (ODbL) is a license agreement intended to allow users to freely share, modify, and use this Dataset while maintaining this same freedom for others, provided that the original source and author(s) are credited.

Link: <https://doi.org/10.3897/jhr.97.119470.suppl1>

Supplementary material 2

PCR primers and conditions used in this study

Author: Hsuan-Pu Chen

Data type: pdf

Explanation note: Regarding PCR conditions, 35 cycles were run for *COI* and *18S*, whereas 30 cycles were run for *28S*. Abbreviations: PCR, polymerase chain reaction.

Copyright notice: This dataset is made available under the Open Database License (<http://opendatacommons.org/licenses/odbl/1.0/>). The Open Database License (ODbL) is a license agreement intended to allow users to freely share, modify, and use this Dataset while maintaining this same freedom for others, provided that the original source and author(s) are credited.

Link: <https://doi.org/10.3897/jhr.97.119470.suppl2>

Supplementary material 3

Fasta and Nexus files for the analysis in this study

Authors: Hsuan-Pu Chen, Namiki Kikuchi

Data type: zip

Explanation note: Fasta files containing alignments of all markers analyzed in this study, along with the Nexus file specifically for the optimal partition scheme identified based on the *COI* and concatenated *18S+28S+COI* datasets for the analysis

Copyright notice: This dataset is made available under the Open Database License (<http://opendatacommons.org/licenses/odbl/1.0/>). The Open Database License (ODbL) is a license agreement intended to allow users to freely share, modify, and use this Dataset while maintaining this same freedom for others, provided that the original source and author(s) are credited.

Link: <https://doi.org/10.3897/jhr.97.119470.suppl3>

Supplementary material 4

Complete maximum likelihood trees reconstructed using the *COI*, *28S*, *18S*, and concatenated *18S+28S+COI* datasets

Author: Hsuan-Pu Chen

Data type: pdf

Explanation note: All trees were rerooted using the outgroup *Agriotypus armatus*. The red and blue colors indicate Phaeogenini and Alomyini, respectively. Branch lengths of the phylogenetic trees are proportional to the inferred number of nucleotide substitutions per site, except for the branch of the outgroup *Agriotypus armatus*. Circles on the nodes indicate different SH-aLRT/UFBoot values. Nodal support with an SH-aLRT value of <80% and a UFBoot value of <95% is not shown. Abbreviations: SH-aLRT, SH-like approximate likelihood ratio test; UFBoot, ultrafast bootstrap approximation; XOR, one or the other but not both.

Copyright notice: This dataset is made available under the Open Database License (<http://opendatacommons.org/licenses/odbl/1.0/>). The Open Database License (ODbL) is a license agreement intended to allow users to freely share, modify, and use this Dataset while maintaining this same freedom for others, provided that the original source and author(s) are credited.

Link: <https://doi.org/10.3897/jhr.97.119470.suppl4>